

# Transmission line model of carbon nanotubes: through the Boltzmann transport equation

Fang Zhou(方舟)<sup>†</sup>

School of Microelectronics, Shanghai Jiao Tong University, Shanghai 200240, China

**Abstract:** A transmission line (TL) model of a carbon nanotube (CNT) is analyzed through the Boltzmann transport equation (BTE). With the help of a numerical solution of the BTE, we study the kinetic inductance ( $L_K$ ), quantum capacitance ( $C_Q$ ) and resistivity ( $R_S$ ) of a CNT under a high frequency electric field. Values of  $L_K$  and  $C_Q$  obtained from BTE accord with the theoretical values, and the TL model is verified by transport theory for the first time. Moreover, our results show that the AC resistivity of CNTs deviates from DC, increasing along with shorter electric field wave length. This shows that changes in  $R_S$  in the high frequency condition must be considered in the TL model.

**Key words:** carbon nanotube; transmission line model; transport equation

**DOI:** 10.1088/1674-4926/32/6/062002

**EEACC:** 2570

## 1. Introduction

As an emerging material of interconnects in future ICs, the metallic carbon nanotube (mCNT) has attracted intense research attention in recent years. In previous works, several characteristics of mCNTs used as interconnects, such as impedance, signal delay, and thermal effects, have been studied and compared with Cu interconnects<sup>[1–3]</sup>. These works are primarily based on the lumped transmission line (TL) model first suggested by Burkel<sup>[4, 5]</sup>, as shown in Fig. 1. What calls for our attention is that, despite many works having been done on the basis of the TL model, few have investigated this generally accepted model in any great depth, whether regarding its accuracy, its applicability or its intrinsic physical properties. Nowadays, experiments towards the RF characteristics of CNTs are proving to be difficult due to the high intrinsic impedance of CNTs as well as the influence of huge electrode capacitance<sup>[6, 7]</sup>. Experimental data of  $L_K$  and  $C_Q$  obtained in Ref. [8] do not accord with the theoretical values in the TL model. Considering the difficulties confronted in experiments, further theoretical methods serve as an alternative to examine the TL model and study its merit or demerit. The Boltzmann transport equation (BTE) takes fundamental physics in the transport process into consideration, such as phonon scattering and band structure.

In Ref. [9], the transmission line equation (TLE) of quantum wire is derived from the BTE through analytical deduction, and kinetic inductance ( $L_K$ ) and quantum capacitance ( $C_Q$ ) are analytically derived and expressed. However, in order to obtain direct and concise expressions, their analytical deduction includes certain assumptions and simplifications. Therefore it is not able to fully consider much important physics, such as phonon scattering and charge's non-equilibrium distribution. Analysis of a specific nano-structure in detail is still inaccessible. Considering this limit of analytical study, numerical calculation is capable of carefully treating this physics and can be extended into the AC condition. In this paper, we provide

a numerical method for solving the BTE under excitation of a periodic AC electric field  $F$  and calculating the current profile  $I(x, t)$  in CNTs. Good agreement between the BTE and the TLE is shown; we also obtained values of  $L_K$ ,  $C_Q$  and  $R_S$  by fitting parameters in the TLE. Our results conform to  $L_K$  and  $C_Q$ 's theoretical values, therefore verifying the TL model. Based on numerical results of the BTE,  $R_S$  is shown to deviate from the value in the DC condition, and it depends on the wave length of the electric field.

## 2. Analysis of transmission line model

Reference [9] shows that electrochemical potential  $\phi$ , rather than electrostatic potential  $\varepsilon$ , should be used in the TLE of nano-structure, as the following formula,

$$L_K \frac{\partial I}{\partial t} + RI = -\frac{\partial \phi}{\partial x}, \quad (1)$$

$$C \frac{\partial \phi}{\partial t} = -\frac{\partial I}{\partial x}. \quad (2)$$

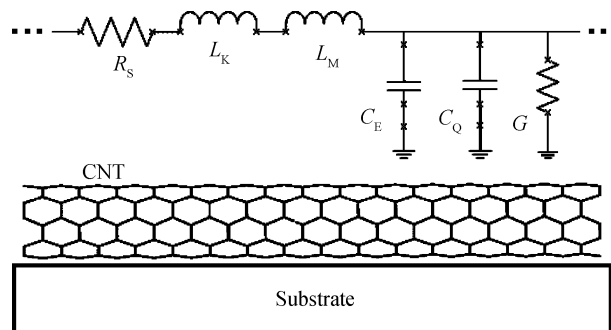


Fig. 1. TL model of a CNT.  $R_S$  is the scattering resistivity,  $G$  is the conductance between the CNT and the substrate,  $L_K$  is the kinetic inductance,  $L_M$  is the magnetic inductance,  $C_Q$  is the quantum capacitance, and  $C_E$  is the electrostatic capacitance.

<sup>†</sup> Corresponding author. Email: fangzhou051@gmail.com

Received 17 November 2010, revised manuscript received 22 December 2010

We neglect magnetic inductance  $L_M$  in Eq. (1) because it is far smaller than  $L_K$  ( $10^{-4}$  times less). This is different from a traditional 3D conductor because of the finite density of state in a quasi-1D nano-structure,  $\phi$  is no longer equal to  $\varepsilon$  and satisfies the relation  $C_E d\varepsilon = C d\phi$ , where  $C$  is the shunt of electrostatic capacitance  $C_E$  and quantum capacitance  $C_Q$ . Equation (1) could be rewritten with  $\varepsilon$  and electric field  $F$  as

$$L_K \frac{\partial I}{\partial t} + RI = -\frac{C_E}{C} \frac{\partial \varepsilon}{\partial t}, \quad (3)$$

$$L_{K|norm} \frac{\partial I}{\partial t} + R_{S|norm} I = -F. \quad (4)$$

We have  $L_{K|norm} = L_K/(1 + C_E/C_Q)$ ,  $R_{S|norm} = R/(1 + C_E/C_Q)$  as normalized  $L_K$  and  $R_S$ . We prefer to use  $\varepsilon$  instead of  $\phi$  in Eq. (4) because  $\varepsilon$  is directly related to  $F$ . The current profile can be calculated from Eq. (4) if the electrical field profile  $F(x, t)$  is known. Next we turn to the BTE to get the numerical relation between  $F$  and  $I(x, t)$ . The BTE can be written as

$$\frac{\partial f}{\partial t} + v_e \frac{\partial f}{\partial x} + v_e e F \frac{\partial f}{\partial E} = \partial_t f_{scat}, \quad (5)$$

where  $v_e$  is the charge velocity. We noticed that the wave velocity of  $F$  is  $v_F = 1/\sqrt{LC}$ .  $L_K$  and  $C_Q$  are decided by band structure and Fermi level, thus  $C_E$  is the main factor responsible for a change in velocity of field in the CNT. So when  $V_F$  changes, equivalently we have changed  $C_E$ , and accordingly the values of  $L_{K|norm}$  and  $R_{S|norm}$  will alter, as in the relation below,

$$L_{K|norm} = \frac{L_K}{1 + 1/(C_Q L_K v^2 - 1)}, \quad (6)$$

$$R_{S|norm} = \frac{R_S}{1 + 1/(C_Q L_K v^2 - 1)}. \quad (7)$$

The resistivity of CNTs ( $R_S$ ) in the DC condition has already been widely studied in many previous works. An analytical expression based on the theory of mean free path (MFP), suggested by Pop in Ref. [10], writes  $R_S$  as

$$R_S = \frac{1}{G_0} \left( \frac{1}{\lambda_e} + \frac{1}{\lambda_{ac}} + \frac{1}{\frac{E_{op}}{Fe} + \lambda_{op}} \right). \quad (8)$$

Equation (8) is derived on the premise that electric field wave length  $\lambda$  is longer than the charge's electric field accelerating length. This assumption becomes really dubious when  $\lambda$  becomes very short (nearly 10 nm). The BTE does not include such an assumption, so  $R_S$  can be studied by BTE free of such restriction. In the following sections,  $R_S$  is shown to deviate from values given by Eq. (8) when  $\lambda$  drastically decreases.

With the numerical method of solving the BTE under periodic electric field  $F(x, t)$ , we could calculate  $I(x, t)$  along the CNT at each time step within a period. Equation (4) gives a relation between  $F(x, t)$  and  $I(x, t)$ . As Eq. (4)'s free parameters, a particular set of  $L_{K|norm}$  and  $R_{S|norm}$  gives the minimum difference of  $I(x, t)$  between the TLE and the BTE. Accordingly  $L_K$ ,  $C_Q$  and  $R_S$  can be calculated by Eqs. (6) and (7), and they fit the results of the BTE.

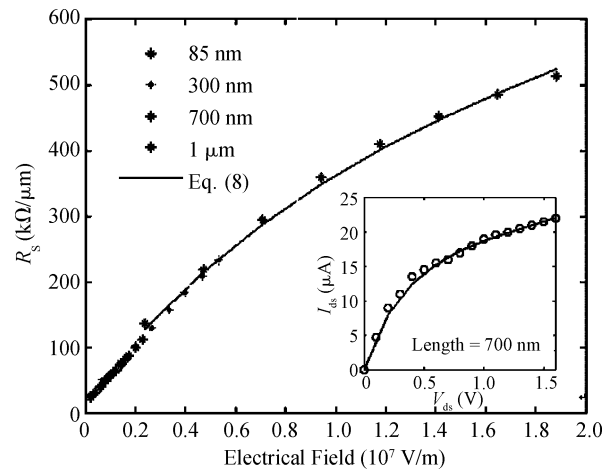


Fig. 2. Resistivity of a CNT under different  $F$ . The solid line is calculated by Eq. (8), and the dots are calculated by the BTE. The length of the CNT changes from 85 nm to 1  $\mu m$ . Equation (8) accords well with the BTE in each case. The inset figure is a comparison between experimental data<sup>[12]</sup> (circle) and calculation of the BTE (solid line).

### 3. Numerical method

We use the method of treating phonon scattering as in Ref. [10]. Scattering terms in the right of Eq. (5) are written as the sum of three terms, separately concerning elastic scattering, forward scattering and backward scattering. They are

$$\partial_t f_{L|e} = (v_e/\lambda_e)(f_R - f_L), \quad (9)$$

$$\partial_t f_{L|pb} = (v_e/\lambda_{pb})[(1 - f_L)f_R^+ - f_L(1 - f_R^-)], \quad (10)$$

$$\partial_t f_{L|pf} = (v_e/\lambda_{pf})[(1 - f_L)f_L^+ - f_L(1 - f_L^-)]. \quad (11)$$

We employ an up-wind difference method similar to Ref. [11] in the numerical calculation. The BTE is solved through integration on time in the DC condition. When it comes to the AC condition, though the field on the CNT varies with time and location, time integration can also determine the correct results when a self-consistent distribution function of electrons  $f(x, E, t)$  is obtained. Before a stable solution is achieved,  $f(x, E, t)$  in the last time step of the previous period serves as the initial value of the next period. A stable solution of  $f(x, E, t)$  is achieved when the difference of two adjacent periods is less than the permitted error. A stable current profile along the CNT in each time step can be obtained from  $I(x, t) = (4e/h) \int f(x, E, t) dE$ .

First we solve  $R_S$  in DC through the BTE. Figure 2 shows that our calculation accords well with experimental data in Ref. [12], and Equation (8) accords well with the results of the BTE. Then we turn to the AC case. An example of solving the BTE under an AC field is shown in Fig. 3. The length of the CNT  $L$  and  $\lambda$  is 1  $\mu m$  in both cases. In numerical calculation,  $L$  is discretized into 100 sections and the period ( $10^{-13}$  s) of  $F$  is discretized into 100 steps. Figure 3(a) plots  $I(x, t)$  calculated from the BTE in each location and time step, Figure 3(b) gives the result solved from Eq. (4), and Figure 3(c) gives their

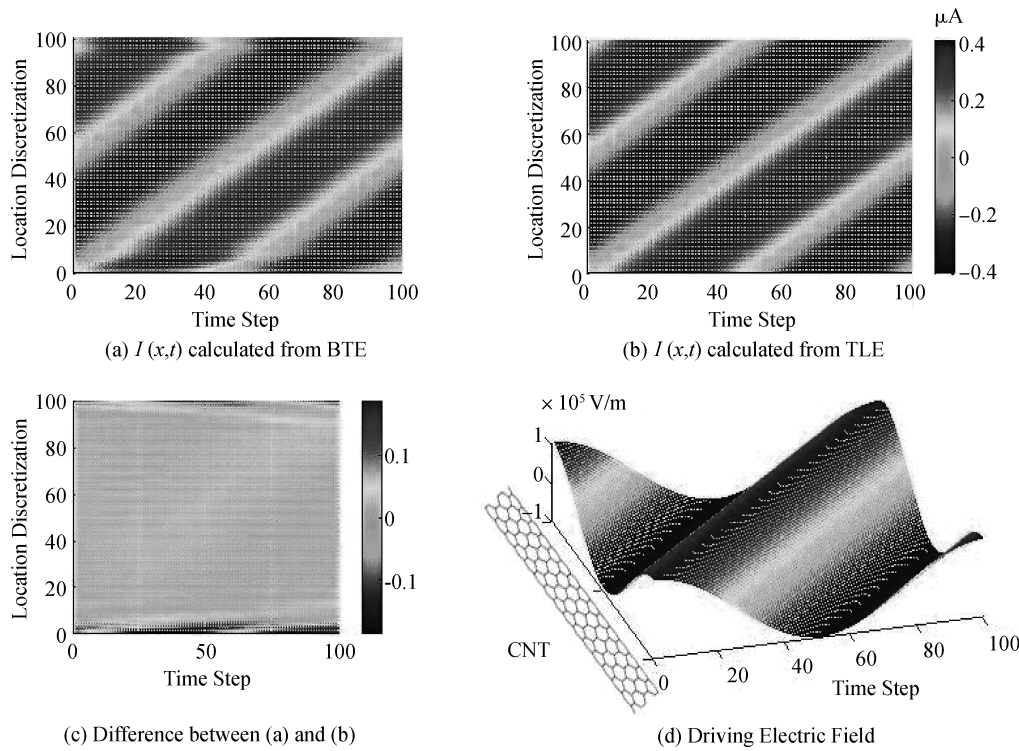


Fig. 3. An example of the numerical solution of the BTE. In our numerical calculation, the CNT length is discretized into 100 sections and the field period is discretized into 100 steps. The electric field  $F$  is of a sin function form with  $\lambda = 1 \mu\text{m}$ ,  $T = 10^{-13} \text{ s}$  and amplitude of  $10^5 \text{ V/m}$ , as shown in (d). (a) and (b) show a full  $I(x, t)$  calculated by the BTE and the TLE, respectively.  $I(x, t)$  also has a sin form as  $F(x, t)$ , whereas a phase shift happens due to  $L_K$ . The difference between the BTE and TLE solutions is plotted in (c), and except for two contact parts of the CNT, a very small difference can be achieved by adjusting the free parameters in Eq. (4).

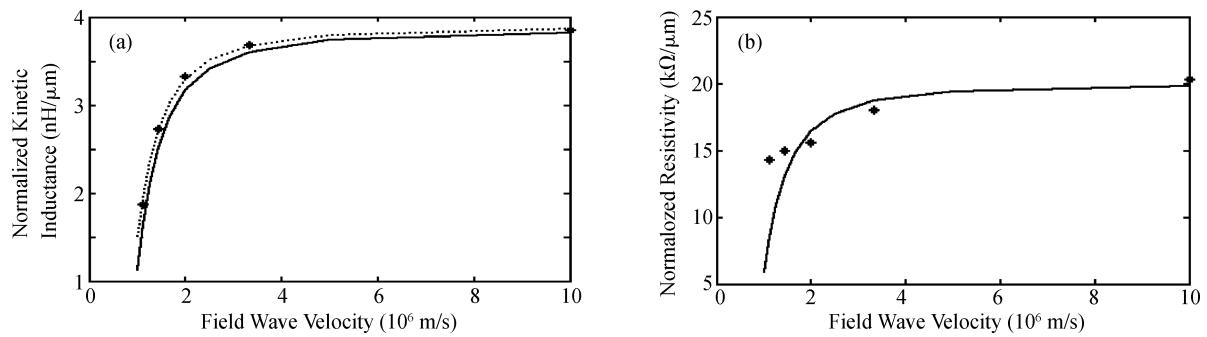


Fig. 4. (a) The solid curve gives values of  $L_{K|\text{norm}}$  from Eq. (6), the dots indicate results from the BTE and the dashed curve is results from Eq. (6) using  $L_K = 3.89 \text{ nH}/\mu\text{m}$ ,  $C_Q = 420 \text{ aF}/\mu\text{m}$  as the best fit. (b) The solid curve gives  $R_{S|\text{norm}}$  from Eq. (6) and the dots are results from the BTE.

Table 1. Fitting results of BTE ( $\lambda = 1 \mu\text{m}$ ).

$V_F$ ( $10^7 \text{ m/s}$ )	$T$ ( $10^{-13} \text{ s}$ )	$C_E$ ( $\text{aF}/\mu\text{m}$ )	$R_{S \text{norm}}$ (BTE) ( $\text{k}\Omega/\mu\text{m}$ )	$L_{K \text{norm}}$ (BTE) ( $\text{nH}/\mu\text{m}$ )
1	1	2.6	20.3	3.85
1/3	3	4.9	17.0	3.68
1/5	5	78.8	15.6	3.33
1/7	7	194.6	15.0	2.73
1/9	9	491.2	14.3	1.87

Table 2. Fitting results of BTE ( $\lambda = 1/9 \mu\text{m}$ ).

$V_F$ ( $10^7 \text{ m/s}$ )	$T$ ( $10^{-13} \text{ s}$ )	$C_E$ ( $\text{aF}/\mu\text{m}$ )	$R_{S \text{norm}}$ (BTE) ( $\text{k}\Omega/\mu\text{m}$ )	$L_{K \text{norm}}$ (BTE) ( $\text{nH}/\mu\text{m}$ )
1	1/9	2.6	40	3.84
2/3	1/6	5.9	39	3.83
1/3	1/3	24.9	37	3.65
1/6	2/3	125.4	30	2.93
1/9	1	491.2	25	1.70

relative difference. We can see that the difference between the result from the BTE and Equation (4) is very small in most locations within a period. Those errors mainly exist in the two

contacts of the CNT, because the BTE model treats the contact as a charge source and it is in equilibrium distribution, so an inexact current profile is obtained.

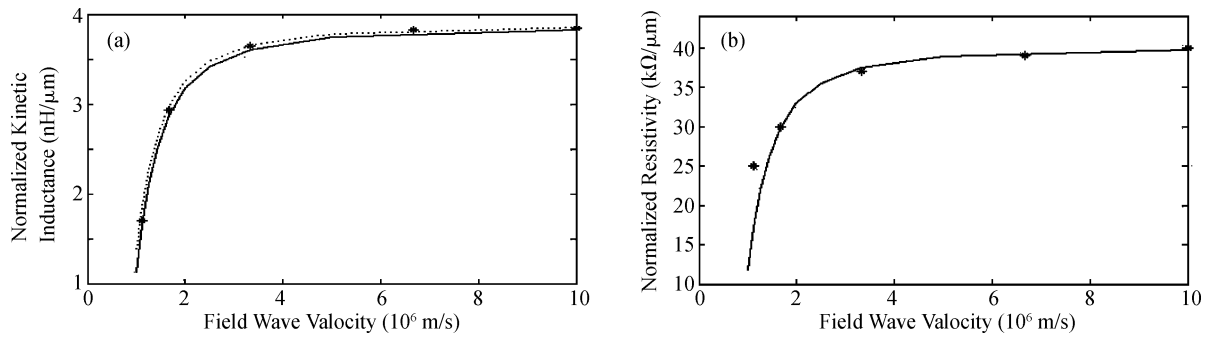


Fig. 5. (a) Solid curve shows values of  $L_{K|norm}$  from Eq. (6), dots indicate results from the BTE and the dashed curve is results from Eq. (6) using  $L_K = 3.88 \text{ nH}/\mu\text{m}$ ,  $C_Q = 400 \text{ aF}/\mu\text{m}$  as the best fit. (b) The solid curve gives  $R_{S|norm}$  from Eq. (6) and the dots are results of the BTE.

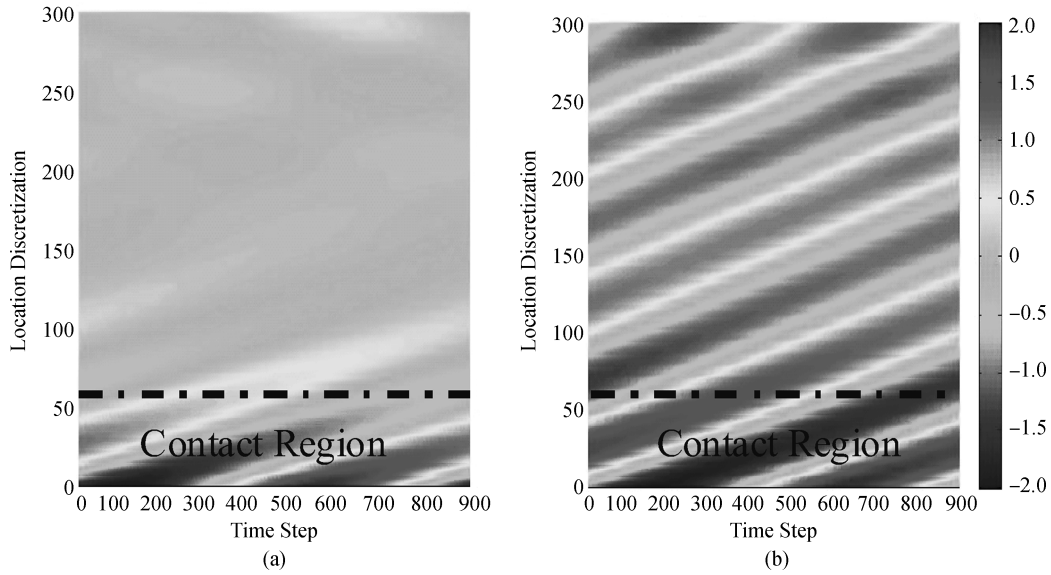


Fig. 6. Difference in  $I(x, t)$  between BTE and TLE along the CNT within a period.  $L_{K|norm} = 1.87 \text{ nH}/\mu\text{m}$ ,  $R_{S|norm} = 14.3 \text{ k}\Omega/\mu\text{m}$ . (a) gives very small difference, however the DC value  $R_{S|norm} = 6 \text{ k}\Omega/\mu\text{m}$ . (b) gives poor accordance. This suggests that under a high frequency and short wave length electric field,  $R_S$  deviates from its DC value.

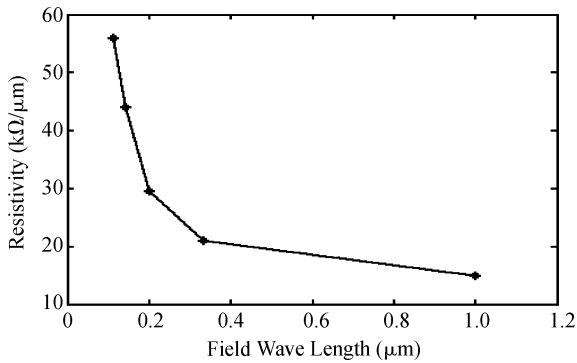


Fig. 7. Relation between  $R_S$  and  $\lambda$ . As  $\lambda$  becomes comparable with the MFP of the electrons,  $R_S$  rapidly rises along with deducing  $\lambda$ .

A limit of the BTE’s application in the AC region is, in order to get the current profile  $I(x, t)$ , electric field profile  $F(x, t)$  must be given ahead.  $F$  should be calculated from the excitation of an external signal source in a more rigorous method. However, if the TL model is accurate enough and equivalent to the BTE, the responding  $I(x, t)$  should be the

same under all kinds of electrical field. This approach can be used to study the TL model under an arbitrary periodic electrical field.

#### 4. Transport simulation

We obtain sets of  $L_{K|norm}$  and  $R_{S|norm}$  under different  $F$  by fitting  $I(x, t)$  of the BTE and the TLE, and they are regarded as BTE results of the BTE.  $F$  has a standard form of sin function as a general condition. Our goal is to verify the generally used value in the TLE,  $L_K = 3.85 \text{ nH}/\mu\text{m}$  and  $C_Q = 368 \text{ aF}/\mu\text{m}$ . Incorporating this value into Eqs. (6) and (7),  $L_{K|norm}$  and  $R_{S|norm}$  can be obtained, and we regard them as results of the TLE. The difference between the BTE and TLE results examines the accuracy of the TL model.

First we use  $\lambda = 1 \mu\text{m}$  longer than the accelerating length of the charge, and period  $T$  changes from  $1 \times 10^{-13}$  to  $9 \times 10^{-13} \text{ s}$ . The calculation results are listed in Table 1. In Figs. 4(a) and 5(a) we found that the fitting values of  $L_{K|norm}$  accord well with theoretical values given by Eq. (6); that is to say that analytical deduction gives identical values of  $L_K$  and  $C_Q$  as the BTE. This establishes the influences of  $L_K$  and  $C_Q$  on

carrier transport in a quasi-1D structure, and identical current profiles with the BTE illustrate that the TL model is effective in considering such effects in the ac condition.

However, fitting value of  $R_S$  does not agree with Eq. (7) well. The BTE results illustrate that  $R_S$  increases when the frequency of  $F$  becomes very high, as shown in Figs. 4(b) and 5(b). The process of fitting would include a certain error. Because of the huge inductive impedance caused by the high frequency,  $R_S$  plays a more subordinate role than  $L_K$ . So very little fluctuation in the current profile is presented when  $R_S$  changes. This leads to inaccuracy of the fitting values of  $R_S$ , and this fluctuation is within  $1 \text{ k}\Omega/\mu\text{m}$  when the fitting process is carefully treated. When  $\lambda = 1 \mu\text{m}$ , we obtained  $R_{S|\text{norm}} = 14.3 \text{ k}\Omega/\mu\text{m}$ , while Equation (7) gives a value of  $6 \text{ k}\Omega/\mu\text{m}$ . The difference in current profile between the BTE and the TLE is illustrated in Fig. 6.  $R_S$  provided by Eq. (7) could not achieve the same current profile as BTE, but fitting  $R_S$  does. This evident deviation of  $R_S$  is out of the region of the fitting fluctuation and should be attributed to a change of  $R_S$  in the high frequency condition.

Then we use an electric field of a shorter wavelength ( $\lambda = 1/9 \mu\text{m}$ ) in order to study the influence of  $\lambda$  on  $R_S$ . This very short  $\lambda$  is comparable to the acceleration length of the charge. Corresponding results are given in Table 2 and Fig. 5. We can see that when  $\lambda$  is as short as  $1/9 \mu\text{m}$ , the fitting value of  $R_{S|\text{norm}}$  rises to  $40 \text{ k}\Omega/\mu\text{m}$ , much larger than  $R_{S|\text{norm}} = 14.3 \text{ k}\Omega/\mu\text{m}$  when  $\lambda = 1 \mu\text{m}$ . This difference indicates the influence of wavelength of field on the CNT's resistivity. To investigate the relation between  $R_S$  and  $\lambda$ , we have a constant period  $T = 10^{-13} \text{ s}$ , and their wavelengths change from  $1/9$  to  $1 \mu\text{m}$ , as illustrated in Fig. 7.  $R_S$  increases evidently when  $\lambda$  is drastically reduced.

## 5. Conclusion

For a CNT interconnect operated in high frequency condition, the expression associating  $F(x, t)$  and  $I(x, t)$  (Eq. (4)) becomes different from the traditional TLE, due to current phase delay caused by  $L_K$ , and the difference between electrochemical and electrostatic potential caused by  $C_Q$ . A numerical method of solving the Boltzmann transport equation un-

der periodic electric field  $F$  is presented. Based on numerical calculation of the BTE, we verify Eq. (4) by introducing two terms,  $L_{K|\text{norm}}$  and  $R_{S|\text{norm}}$ , which incorporate the effects of  $C_Q$  into the TLE (Eqs. (6) and (7)).  $L_K$  and  $C_Q$  calculated by the BTE accord well with theoretical values in the TL model.  $R_S$  is shown to change with field wave length. More work is needed for further study of the CNT's resistivity under high frequency field, especially when wave length becomes comparable to the charge's MFP. The TL model must take changing  $R_S$  into consideration to address concerns about accuracy.

## References

- [1] Srivastava N, Li H, Kreupl F, et al. On the applicability of single-walled carbon nanotubes as VLSI interconnects. *IEEE Trans Nanotechnol*, 2009, 8(4): 542
- [2] Li H, Yin W Y, Banerjee K, et al. Circuit modeling and performance analysis of multi-walled carbon nanotube interconnects. *IEEE Trans Electron Devices*, 2008, 55(6): 1328
- [3] Pop E, Mann D A, Goodson K E, et al. Electrical and thermal transport in metallic single-wall carbon nanotubes on insulating substrates. *J Appl Phys*, 2007, 101(9): 093710
- [4] Burke P J. Luttinger liquid theory as a model of the Gigahertz electrical properties of carbon nanotubes. *IEEE Trans Nanotechnol*, 2002, 1(3): 129
- [5] Burke P J. An RF circuit model for carbon nanotubes. *IEEE Trans Nanotechnol*, 2003, 2(1): 55
- [6] Li S D, Yu Z, Yen S F, et al. Carbon nanotube transistor operation at 2.6 GHz. *Nano Lett*, 2004, 4(4): 753
- [7] Gomez-Rojas L, Bhattacharyya S, Mendoza E, et al. RF response of single-walled carbon nanotubes. *Nano Lett*, 2007, 7(9): 2672
- [8] Nougaret L, Dambrine G, Lepilliet S, et al. Gigahertz characterization of a single carbon nanotube. *Appl Phys Lett*, 2010, 96(4): 042109
- [9] Salahuddin S, Lundstrom M, Datta S. Transport effects on signal propagation in quantum wires. *IEEE Trans Electron Devices*, 2005, 52(8): 1734
- [10] Yao Z, Kane C L, Dekker C. High-field electrical transport in single-wall carbon nanotubes. *Phys Rev Lett*, 2000, 84(13): 2941
- [11] Aksamija Z, Ravaioli U. Boltzman transport simulation of single-walled carbon nanotubes. *J Comput Electron*, 2008, 7: 315
- [12] Javey A, Guo J, Paulsson M, et al. High-field, quasi-ballistic transport in short carbon nanotubes. *Phys Rev Lett*, 2004, 92: 106804